

## Electronic supplementary information

# MOF Nanoparticles with Encapsulated Dihydroartemisinin in Controlled Drug Delivery System for Enhanced Cancer Therapy and Mechanism Analysis

Yawei Li, Yu Song, Wei Zhang, Junjie Xu, Jiancheng Hou, Xianmin Feng\* and Wenhe Zhu\*

## Experimental Section

### Materials and methods

All starting chemicals and solvents were purchased from commercial sources and used without further treatment, unless indicated otherwise. FTIR was measured by Nicolet Impact 410 Fourier transform infrared spectrometer. UV was recorded on SHIMADZU UV-2450 spectrometer. TEM and SEM images were recorded by JEOL JEM-1011 electron microscope (acceleration voltage of 100 kV) and JEOL JXA-840 (acceleration voltage of 15 kV). Size and zeta potential were measured by Malvern Zeta Sizer-Nano ZS90 instrument. PXRD was performed by a Rigaku D/MAX2550 diffractometer using CuK $\alpha$  radiation, 40 kV, 200 mA with scanning rate of 0.4 ° min<sup>-1</sup>. TGA was performed using a NetzchSta 449c thermal analyzer system at a rate of 10 °C min<sup>-1</sup> under air atmosphere.

### One-pot Synthesis of MOFs

In a typical experiment, 75 mg of zinc nitrate hexahydrate was dissolved in 2.5 mL of deionized water, on the other hand, 165 mg of 2-methyl imidazole was dissolved into 4.5 mL of methanol and 10 mg of DHA was dissolved into 0.5 mL of DMF. Under stirring, the aqueous of zinc nitrate was added into the solution of 2-methyl imidazole and DHA at room temperature, the synthesis solution quickly turned turbid. After 3 min, DHA@ZIF-8 NPs were formed. The solution was centrifuged at 12000 rpm for 10 min to obtain the DHA@ZIF-8 NPs. Then DHA@ZIF-8 NPs was washed with methanol three times to completely remove the unreacted reagents. The supernatants were all collected for the measurement of encapsulation efficiency and drug loading content of DHA. The DHA in the supernatant was converted into a UV absorbing compound through treatment with 0.2% NaOH aqueous solution at 50°C for 30 min and the detection wavelength was 290 nm by the UV-vis spectrometer. Finally, the products were freeze-dried and stored at -20 °C until further use. As a control, ZIF-8 NPs were synthesized with the same method.

### Cell culture

The human HCC cell lines (HepG2, SMMC-7721 and BEL-7404) and normal hepatocytes (HL-7702) were routinely grown in DMEM medium and cultured in medium containing 10% fetal bovine serum (FBS) and 1% penicillin/streptomycin at 37 °C under 5% CO<sub>2</sub>.

### Cellular Uptake

Cellular uptakes by HepG2 cells were examined using a confocal laser scanning microscope (CLSM). Cells were seeded in 6-well culture plates (a sterile cover slip was put in each well) at a density of 5×10<sup>4</sup> cells per well and allowed to adhere for 24 h. After that, the cells were treated with DHA@ZIF-8 NPs (20 μM) for 0.5 h at 37 °C. Thereafter cells were incubated for additional 0.5 h, 2 h, and 4 h at 37 °C. Subsequently, the supernatant was carefully removed and the cells were washed three times with PBS. Subsequently, the cells were fixed with 500 μL

of 4% formaldehyde in each well for 20 min at room temperature and washed twice with PBS again. Cells were visualized using blue channel for Hoechst 33258 and red channel for NR under a confocal laser scanning microscope (Carl Zeiss LSM 700).

### **Cytotoxicity Test**

The cytotoxicity test was measured via MTT assay. HepG2, SMMC-7721, BEL-7404 or HL-7702 cells harvested in a logarithmic growth phase were seeded in 96-well plates at a density of  $10^5$  cells/well and incubated in DMEM for 24 h. The medium was then replaced by DHA or DHA@ZIF-8 NPs, at a final equivalent DHA concentration from 10 to 100  $\mu$ M for each drug. The incubation was continued for 24 h. Then, 20  $\mu$ L of MTT solution in PBS with the concentration of 5 mg/mL was added and the plates were incubated for another 4 h at 37 °C, followed by removal of the culture medium containing MTT and addition of 150  $\mu$ L of DMSO to each well to dissolve the formazan crystals formed. Finally, the plates were shaken for 10 min, and the absorbance of formazan product was measured at 490 nm by a microplate reader. Each data point was an average of three independent experiments.

### **Apoptosis**

The apoptosis and necrosis induced by DHA@ZIF-8 NPs were evaluated by flow cytometry. HepG2 cells treated with different concentrations of DHA@ZIF-8 NPs were harvested by centrifugation at 1000 rpm for 5 min, and washed with ice-cold PBS. The cell suspension (100  $\mu$ L) was centrifuged at 1000 rpm for 5 min. After that, the supernatant was discarded and the pellet was gently resuspended in 195  $\mu$ L annexin V-FITC binding buffer, and incubated with 5  $\mu$ L propidium iodide (PI) solution on an ice bath in the dark. After filtration (300  $\mu$ m), the suspension from each group was analyzed using a flow cytometry.

### **Total RNA extraction and mRNA Library Construction**

Total RNA was extracted from the cells DHA@ZIF-8 NPs treated or control cells using Trizol (Invitrogen, Carlsbad, CA, USA) according to manual instruction. Total RNA was qualified and quantified using a Nano Drop and Agilent 2100 bioanalyzer (Thermo Fisher Scientific, MA, USA).

Oligo(dT)-attached magnetic beads were used to purified mRNA. Purified mRNA was fragmented into small pieces with fragment buffer at appropriate temperature. Then First-strand cDNA was generated using random hexamer-primed reverse transcription, followed by a second-strand cDNA synthesis. Afterwards, A-Tailing Mix and RNA Index Adapters were added by incubating to end repair. The cDNA fragments obtained from previous step were amplified by PCR, and products were purified by Ampure XP Beads, then dissolved in EB solution. The product was validated on the Agilent Technologies 2100 bioanalyzer for quality control. The double stranded PCR products from previous step were heated denatured and circularized by the splint oligo sequence to get the final library. The single strand circle DNA (ssCir DNA) was formatted as the final library. The final library was amplified with phi29 to make DNA nanoball (DNB) which had more than 300 copies of one molecular, DNBS were loaded into the patterned nanoarray and single end 50 bases reads were generated on BGISEQ500 platform (BGI-Shenzhen, China).

### **Bioinformatics Methods**

The sequencing data was filtered with SOAPnuke (v1.5.2) by removing reads containing sequencing adapter. The clean reads were mapped to the reference genome using HISAT2 (v2.0.4). Bowtie2 (v2.2.5) was applied to align the clean reads to the reference coding gene set, then expression level of gene was calculated by RSEM (v1.2.12). The heatmap was drawn by pheatmap (v1.0.8) according to the gene expression in different samples. Essentially, differential expression analysis was performed using the DESeq2 (v1.4.5) with Q value  $\leq$  0.05. To take insight to the change of phenotype, GO and KEGG enrichment analysis of annotated different expressed gene was performed by Phyper based on Hypergeometric test. The significant levels of terms and pathways were corrected by Q value with a rigorous threshold (Q value  $\leq$  0.05) by Bonferroni.

### **Western blot and antibodies**

Western blotting was performed using standard methods. After being treated with different concentrations of DHA@ZIF-8, the cell pellets were suspended in radio immunoprecipitation assay buffer (150 mM sodium chloride, 50 mM Tris pH 8.0, 1% Triton X-100, 0.5% sodium deoxycholate, 0.1% SDS) supplemented with 10 mM NaF, 1mM  $\text{Na}_3\text{VO}_4$ , 5 mM EDTA, 1 mM EGTA, 5 mg/ml leupeptin, 1 mg/ml pepstatin A, 1 mM phenyl methylsulfonyl fluoride, and protease and phosphatase inhibitor for 15 min at 4 °C and centrifuged at 12000 rpm 20 min at 4 °C. Protein concentration of the supernatants was determined using a BCA protein Assay Kit (Beyotime Biotechnology, China). Equal amounts (50  $\mu\text{g}$ ) of the proteins were resolved by 12% SDS-polyacrylamide gel electrophoresis gels and transferred to PVDF membranes (Millipore) using a Bio-Rad Trans-blot instrument. Membranes were blocked in 5% milk for 1 h at room temperature following incubation with the indicated primary antibody overnight at 4 °C, washed 3 times with TBS-T buffer, incubated with secondary antibody IgG-HRP at 1:20000 dilutions in TBS-T buffer (Cat. #A11034 for anti-rabbit; Cat. #A-32723 for anti-mouse by Invitrogen). After washing 3 times with TBS-T buffer, the membrane was developed with ECL substrate (Thermo Scientific) and the signal was detected by a BIO-RAD Fluorescent Imager, following quantification by Image Lab software.

The following antibodies were used in this study, all diluted in TBS-T including 3% milk. Antibodies directed against, P-AKT (ab18622), AKT (ab32505), P53 (ab26), Cleaved Caspase-3 (ab32042), Cleaved Caspase-9 (ab2324), Cytochrome C (ab13575), Bax (ab32503), Bcl-2 (ab32124) were obtained from Abcam (1:1 000 dilution), p-mTOR (sc-293089), mTOR (sc-517464), HIF-1 $\alpha$  (sc-13515), Glut1(sc-377228),  $\beta$ -actin (23660-1-AP) were obtained from proteintech (1:5 000 dilution).

### ***In vivo* antitumor test and safety evaluation**

All the experimental procedures to mouse described herein have gained approval from the Ethics Committee of Jilin Medical University and carried out corresponding to the regulation, principles, and guidelines of Chinese law concerning the protection of animal life. Kunming (KM) female mice were obtained from Jilin University and maintained under required conditions. The H22 xenograft tumor models were established by injecting H22 hepatocellular carcinoma cells into the left infra-axillary dermis of the mice. When the tumor grew to a size of  $\sim 100 \text{ mm}^3$ , H22 bearing Kunming mice were randomly divided into four groups with 4 mice in each group: Control, ZIF-8 NPs, free DHA, DHA@ZIF-8 NPs. Mice were administered PBS, ZIF-8 NPs, free DHA or DHA@ZIF-8 NPs with the same dosage of 5 mg /kg DHA via tail vein injection once every 2 days, respectively, and the tumor volume and body weight were measured every other day in 12 days. After 12 days of observation and measurement, the mice of four groups were sacrificed and the tumors were excised to intuitively evaluate the tumor inhibition.

In order to investigate the safety of DHA@ZIF-8 NPs, the potential hepatic and renal toxicity was evaluated. The blood of mice was taken out for testing the level of serum alanine transaminase (ALT), aspartate transaminase (AST), uric acid (UA) and creatinine (CREA). Main organs (heart, liver, spleen, lung, kidney) and tumor were collected, fixed in 4% paraformaldehyde solution, and then embedded in paraffin, sliced and stained with hematoxylin and eosin (H&E) to evaluate potential toxicity for main organs and apoptosis degree for cancer cells.

### **Statistical Analysis**

All experiments were performed at least three times and all results were expressed as mean  $\pm$  standard deviation (SD). Student's t-test was used to determine the statistical difference between various experimental and control groups. Significant differences between the groups are indicated by \* for  $p < 0.05$ , \*\* for  $p < 0.01$ , and \*\*\* for  $p < 0.001$ , respectively.

## Results

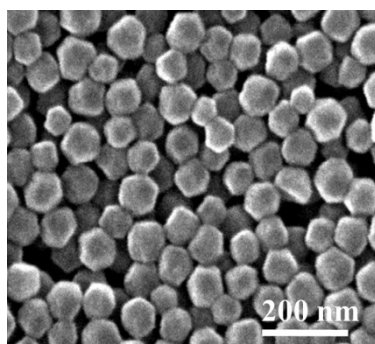


Fig. S1 SEM image of DHA@ZIF-8 NPs.

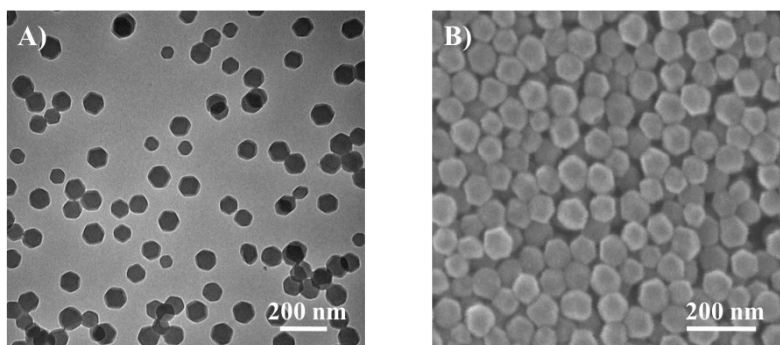


Fig. S2 A) SEM image and B) TEM image of ZIF-8 NPs.

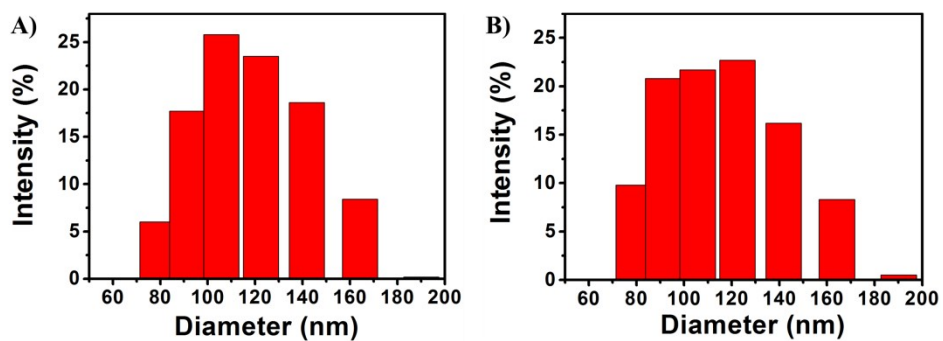


Fig. S3 Particle size distributions of A) ZIF-8 NPs and B) DHA@ZIF-8 NPs dispersed in water.

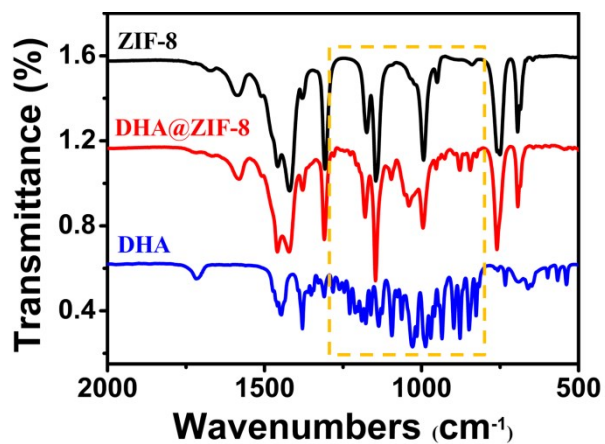


Fig. S4 FTIR spectra of ZIF-8 NPs, DHA@ZIF-8 NPs and free DHA.

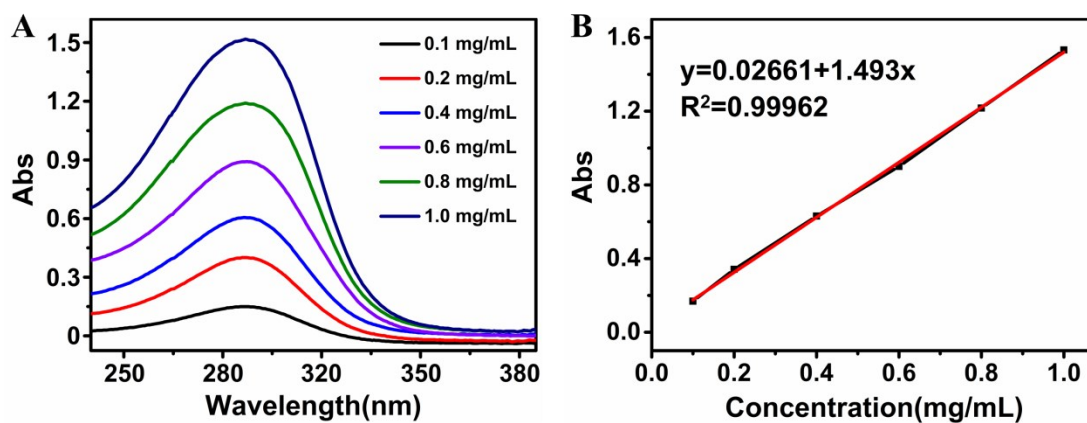


Fig. S5 The quantification of DHA loading by UV-vis spectra. (A) UV-vis absorption curves of DHA solutions with different concentrations. (B) The standard curve for absorbance values at 290 nm.

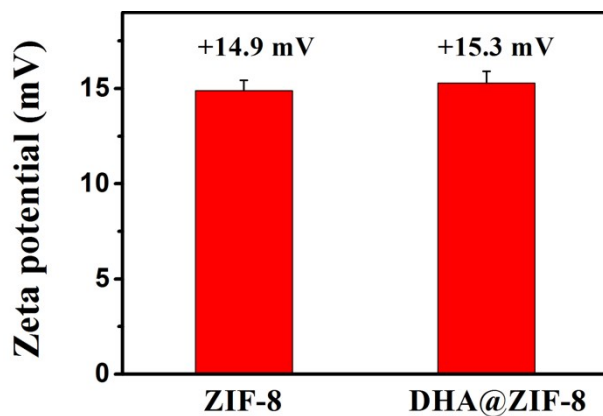
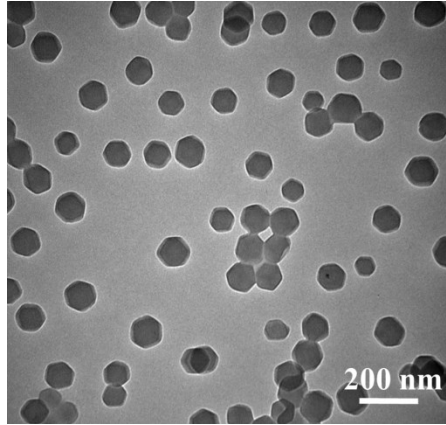
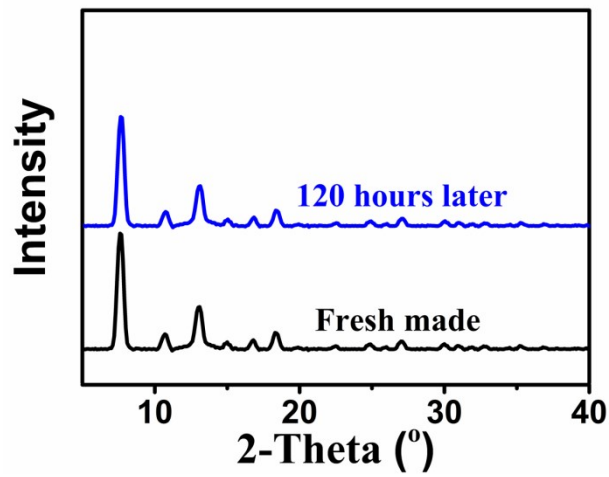


Fig. S6 Zeta potential of ZIF-8 NPs and DHA@ZIF-8 NPs.



**Fig. S7** TEM image of DHA@ZIF-8 NPs after being immersed in PBS with FBS (10%) for 120 h.



**Fig. S8** PXRD of DHA@ZIF-8 NPs which were freshly made and 120 h after being immersed in PBS with FBS (10%).

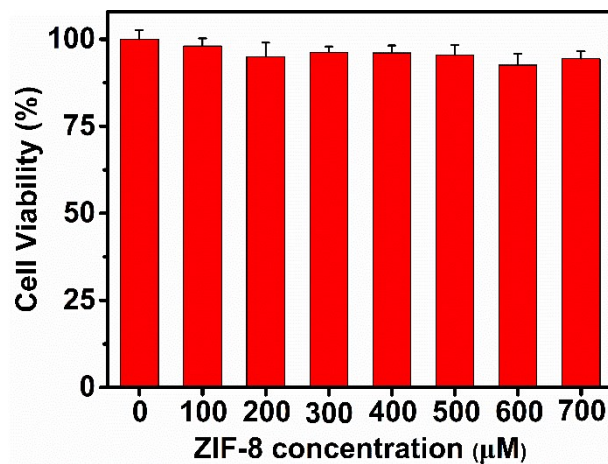


**Fig. S9** Cell viabilities of HL-7702 cells after incubation with various levels of ZIF-8 NPs for 24 h.

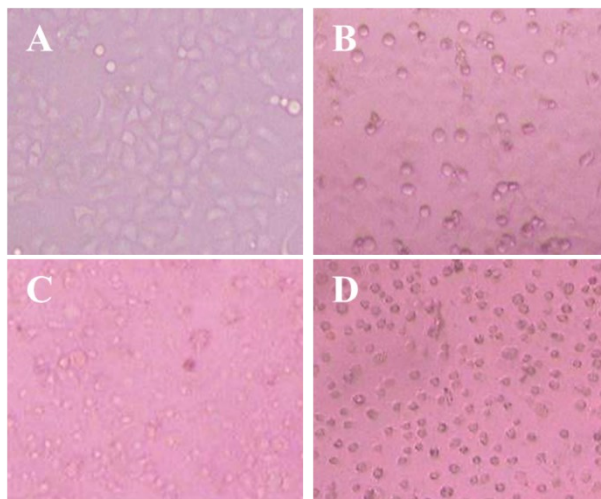


**Fig. S10** The cell morphologies observed by inverted microscope. (A) the control group, (B-D) the groups of different concentrations of DHA@ZIF-8 NPs (20, 40, 60  $\mu\text{M}$ ).

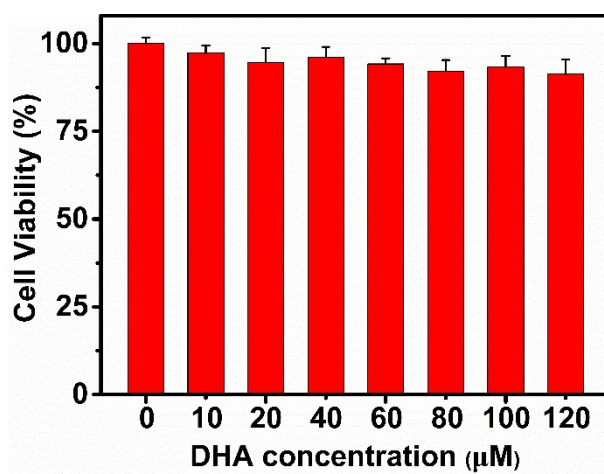


**Fig. S11** Cell viabilities of HL-7702 cells after incubation with various levels of DHA@ZIF-8 NPs for 24 h.

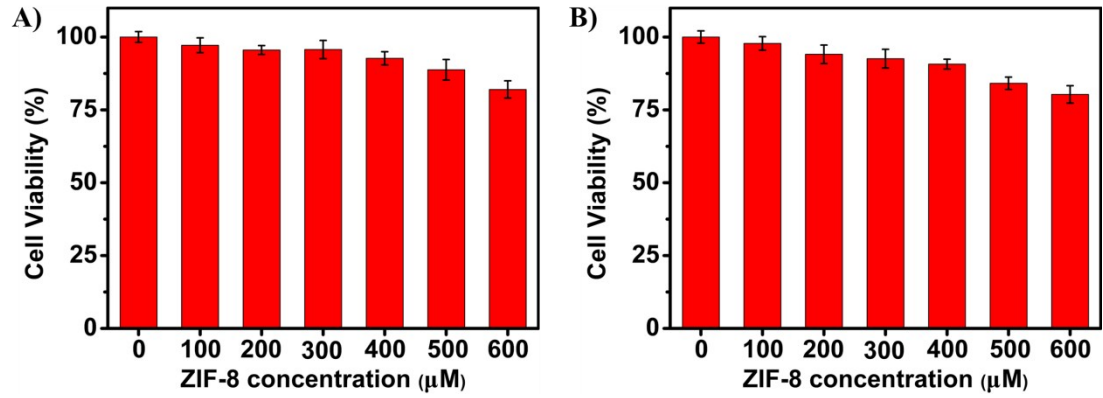


**Fig. S12** *In vitro* biocompatibility of ZIF-8 NPs against A) SMMC-7721 and B) BEL-7404 cells, respectively. Data represent mean values  $\pm$  standard deviation,  $n = 3$ .

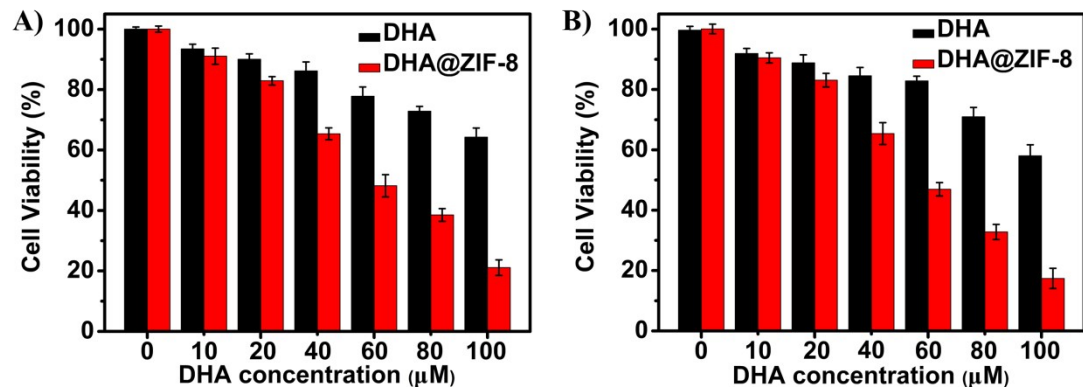


**Fig. S13** *In vitro* cytotoxicities of free DHA and DHA@ZIF-8 NPs against A) SMMC-7721 and B) BEL-7404 cells at different concentrations after 24 h. Data represent mean values  $\pm$  standard deviation,  $n = 3$ .

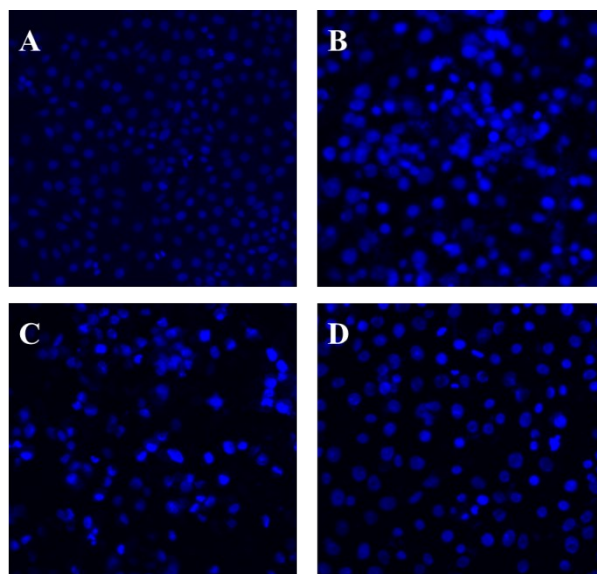


**Fig. S14** Morphological apoptosis in HepG2 cells treated with different concentrations of DHA@ZIF-8 NPs was determined by staining with Hoechst 33258. (A) Control group, (B-D) the groups of different concentrations of DHA@ZIF-8 NPs (20, 40, 60  $\mu$ M).

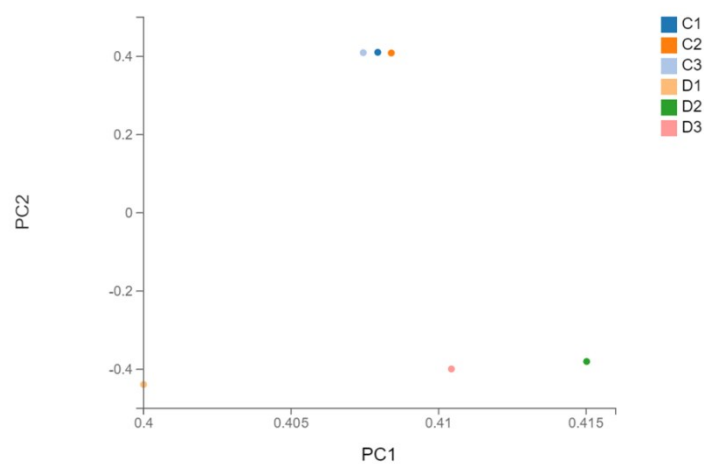


**Fig. S15** Principal component analysis (PCA) of HepG2 cells based on untreated control (C) and DHA@ZIF-8 NPs treatment groups (D).

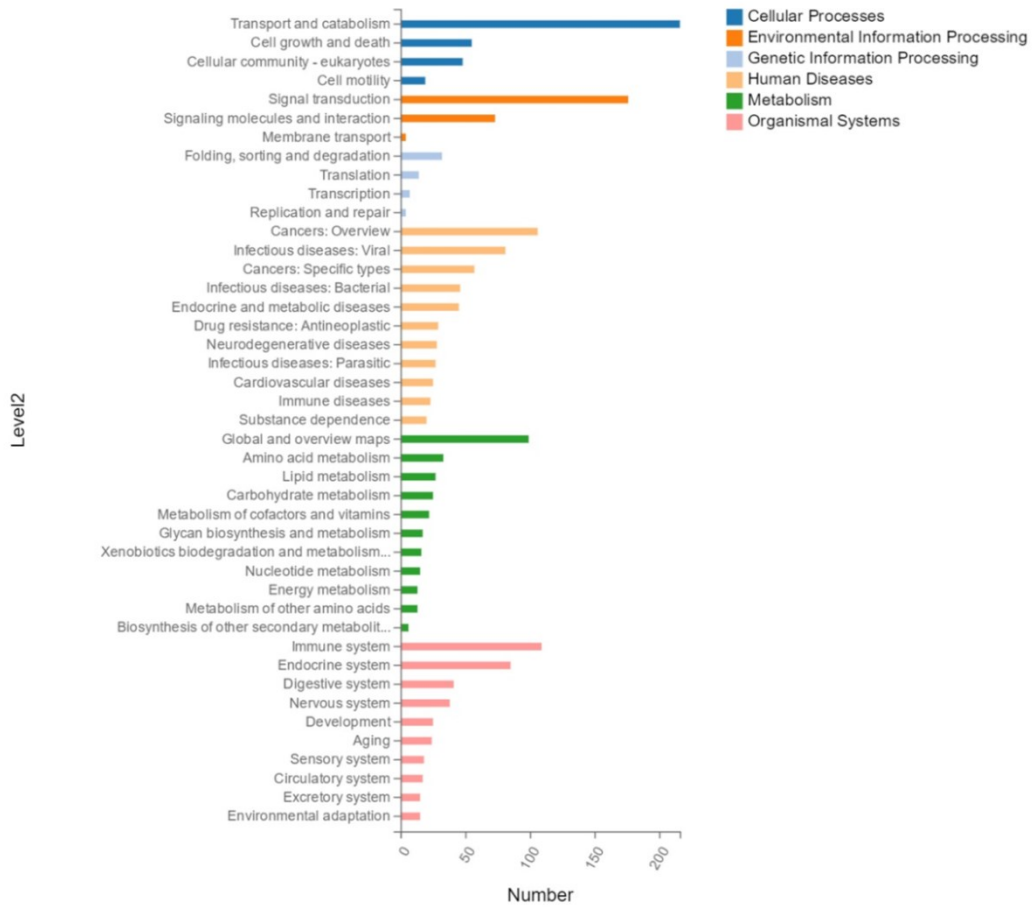


**Fig. S16** KEGG pathway classification of differentially expressed genes (DEGs). X axis represents number of DEGs, Y axis represents functional classification of KEGG.

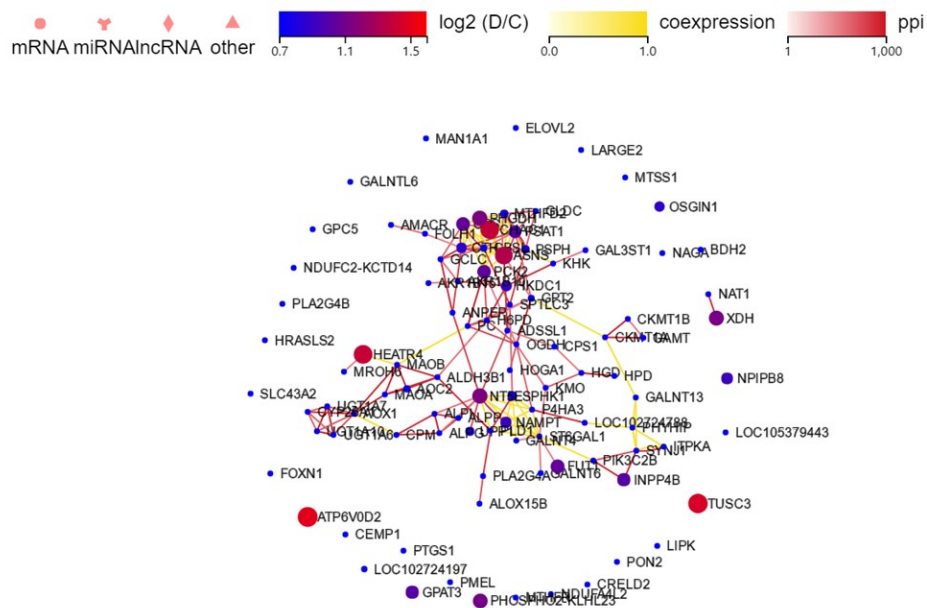


**Fig. S17** PPI network of the DEGs correlation with Metabolism.

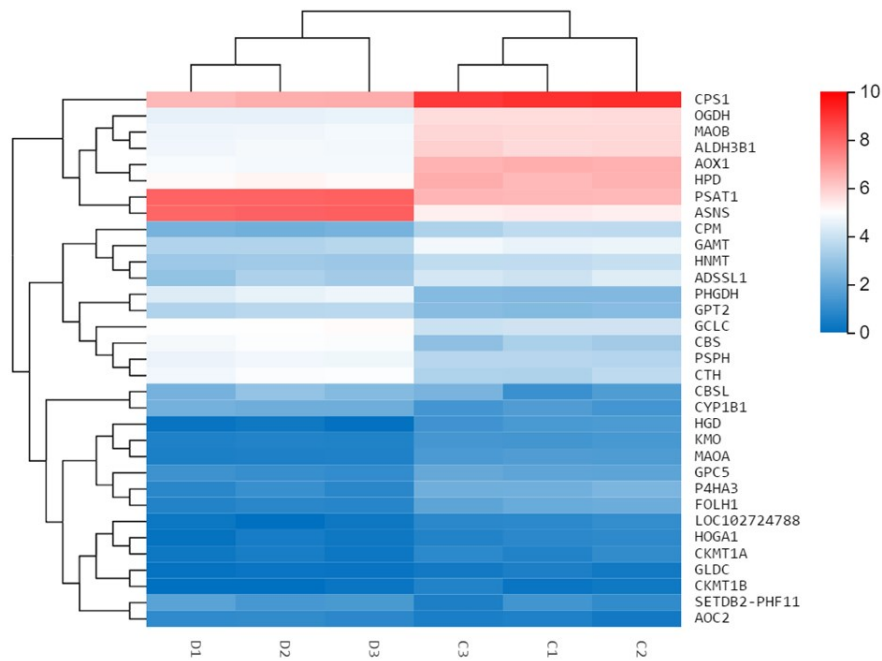


**Fig. S18** Heatmap analysis for the DEGs correlation with amino acid metabolism. Red and blue in the colour bar represent high and low expression levels, respectively. DEGs were analysed between DHA@ZIF-8 NPs group (D) and control group (C).

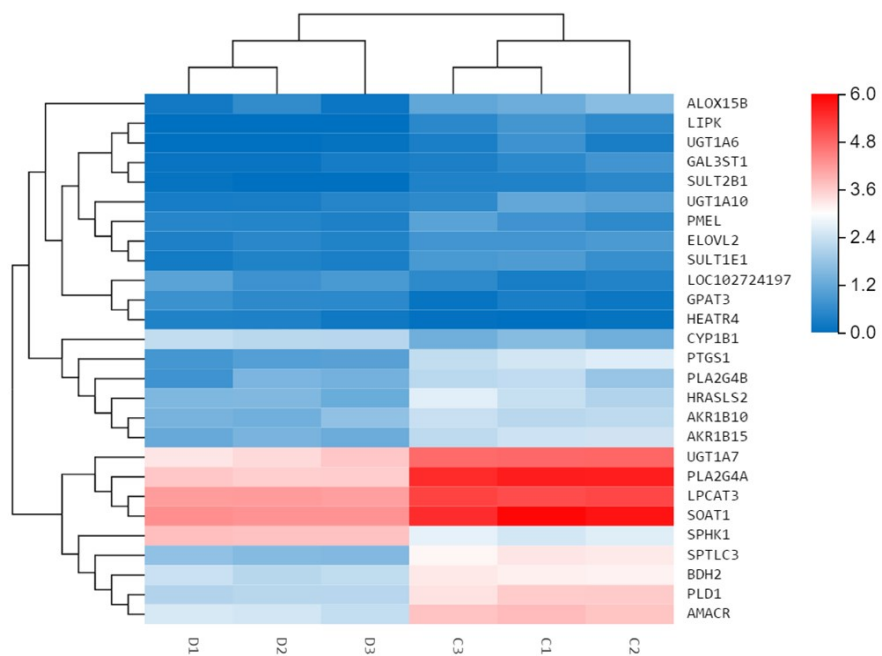


**Fig. S19** Heatmap analysis for the DEGs correlation with lipid metabolism. Red and blue in the colour bar represent high and low expression levels, respectively. DEGs were analysed between DHA@ZIF-8 NPs group (D) and control group (C).

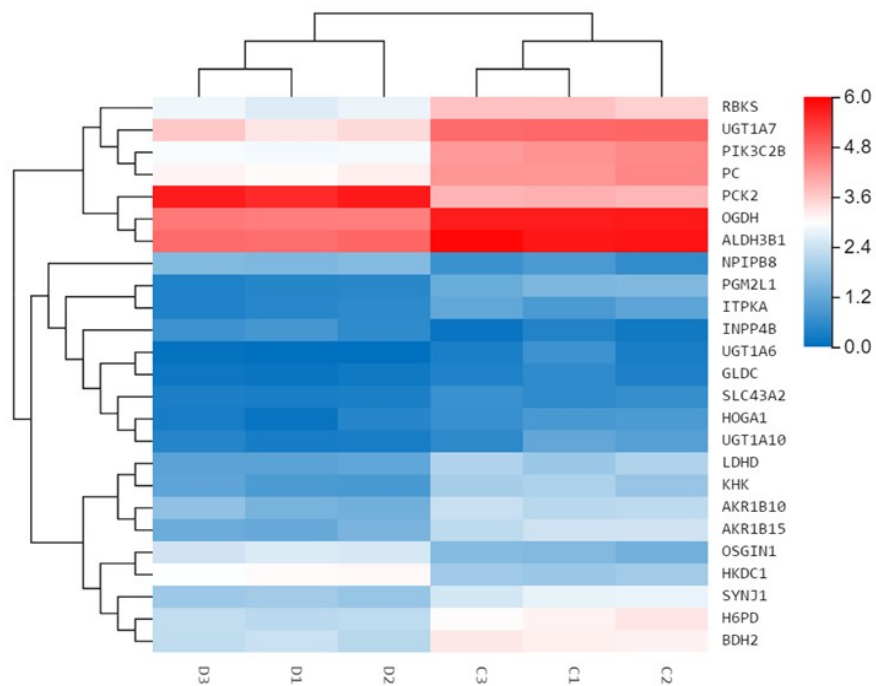


**Fig. S20** Heatmap analysis for the DEGs correlation with carbohydrates. Red and blue in the colour bar represent high and low expression levels, respectively. DEGs were analysed between DHA@ZIF-8 NPs group (D) and control group (C).

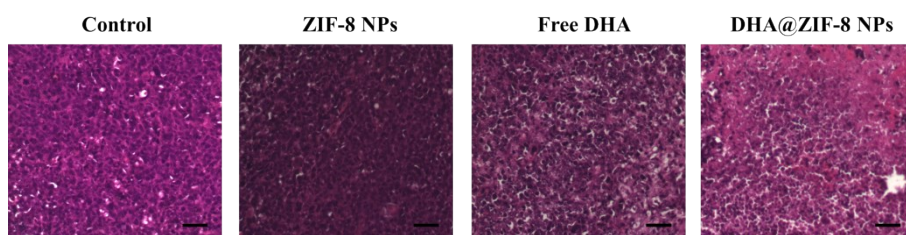


**Fig. S21** H&E staining of tumor regions from tumor-bearing Kunming mice after different treatment. Scale bars: 100  $\mu$ m.

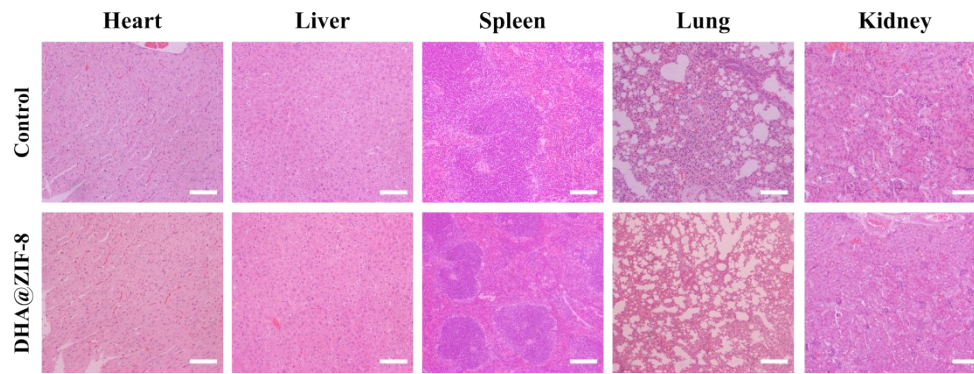


**Fig. S22** H&E staining of different organs (heart, liver, spleen, lung and kidney) of mice in control and DHA@ZIF-8 NPs groups. Scale bars: 100  $\mu\text{m}$ .

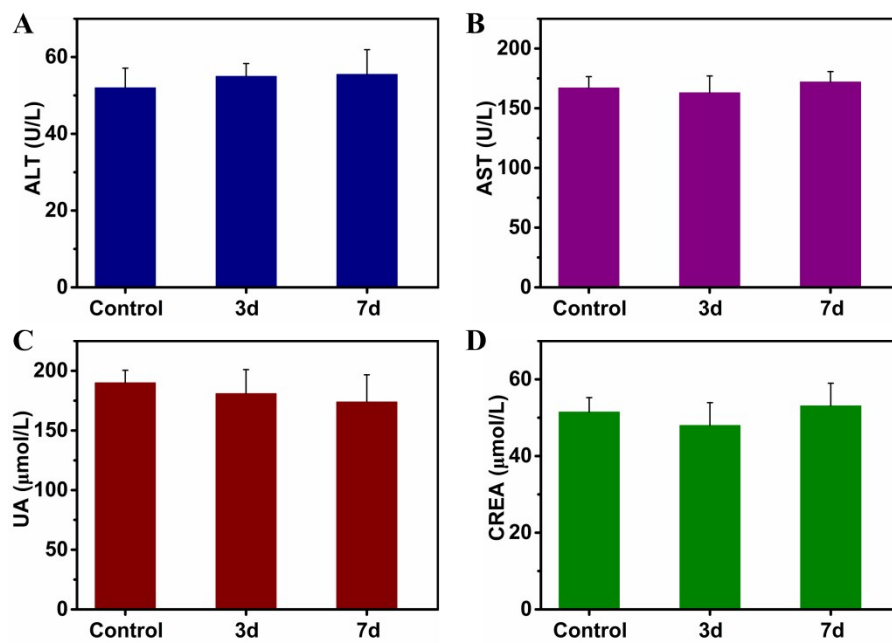


**Fig. S23** Serum biochemistry analysis of kidney and liver function parameters after DHA@ZIF-8 NPs treatment. (A) alanine transaminase (ALT), (B) aspartate aminotransferase (AST), (C) uric acid (UA), and (D) creatinine (CREA). Data represent mean values  $\pm$  standard deviation,  $n = 4$ .